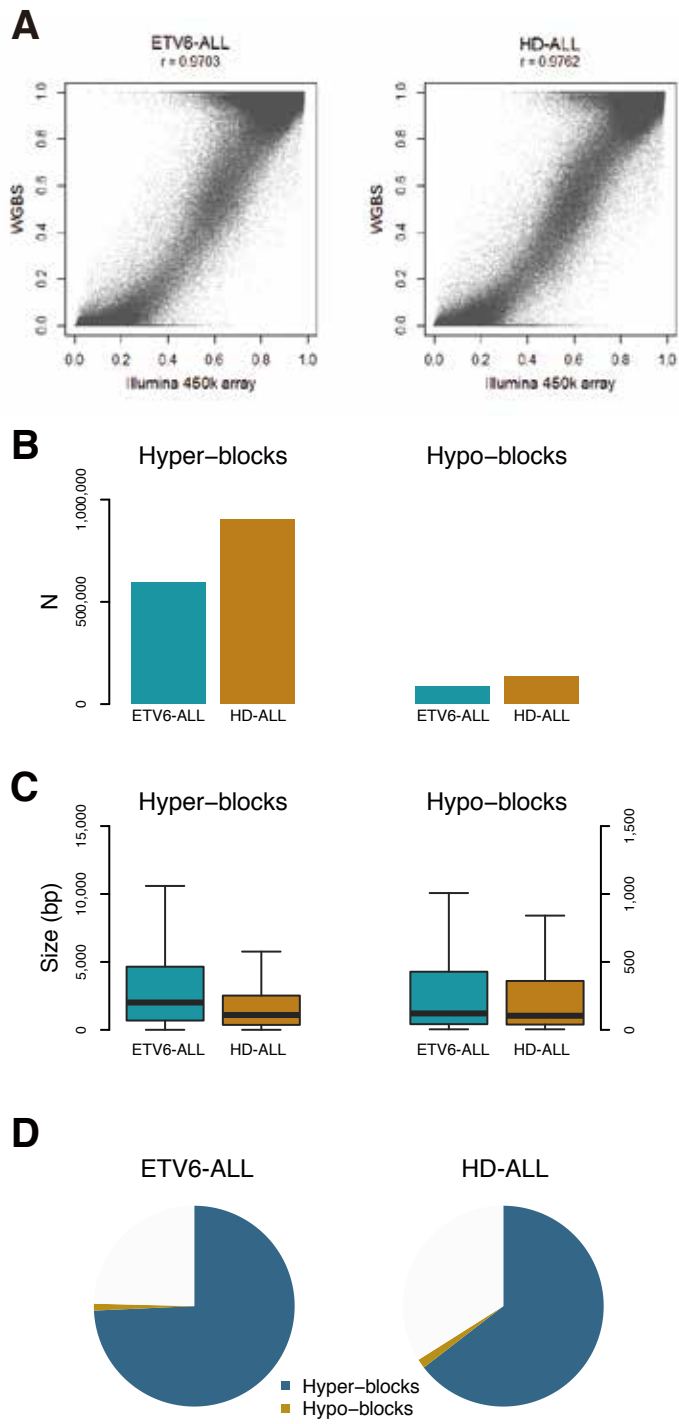


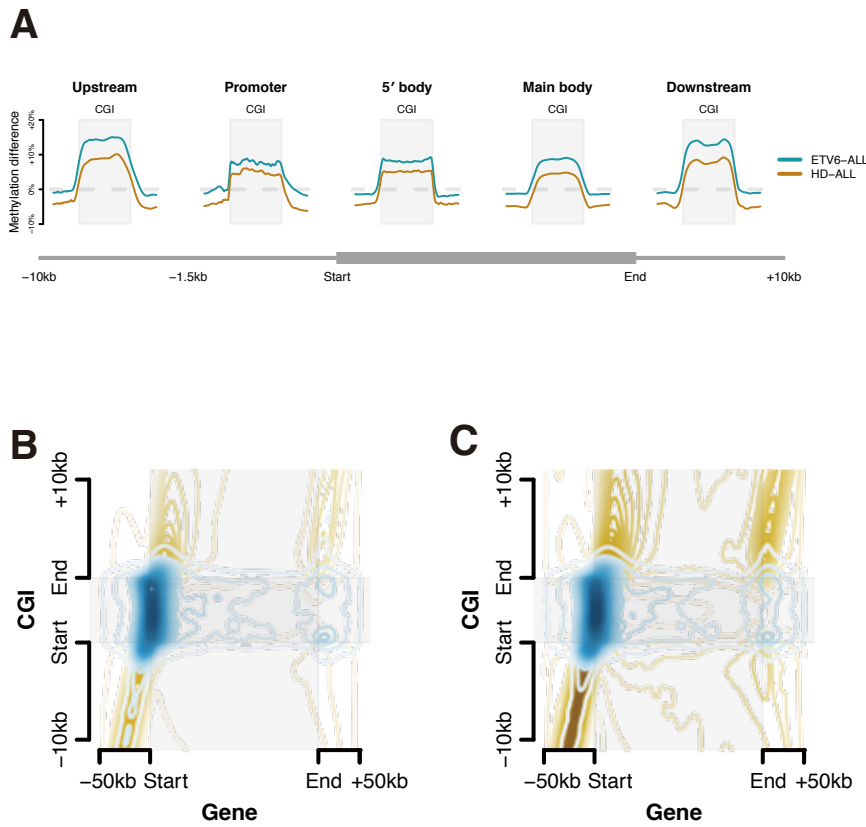
Supplemental Figure S1



Statistics of whole genome bisulfite sequencing (WGBS)

- (A) Comparison of whole genome bisulfite sequencing (WGBS) and Illumina 450k array data demonstrates high correlation ($r > 0.9$).
- (B) Statistics of methylation blocks in ETV6-ALL and HD-ALL. Hyper-blocks are defined as regions with $\geq 75\%$ methylation and hypo-blocks with $\leq 25\%$ in consecutive CpGs. HD-ALL has larger numbers of hyper- and hypomethylated blocks (865,743 and 128,846, respectively) than ETV6-ALL (578,413 and 84,157, respectively).
- (C) HD-ALL has smaller sizes of hyper- and hypomethylated blocks (median: 1,095 and 104 bp, respectively) than ETV6-ALL (median: 2,013 and 121 bp, respectively).
- (D) Collectively, hyper-blocks in ETV6-ALL cover much larger genomic regions (2,140,398,701 bp; 74.3% of whole autosomes) than HD-ALL (2,140,398,701 bp; 64.5% of whole autosomes).

Supplemental Figure S2

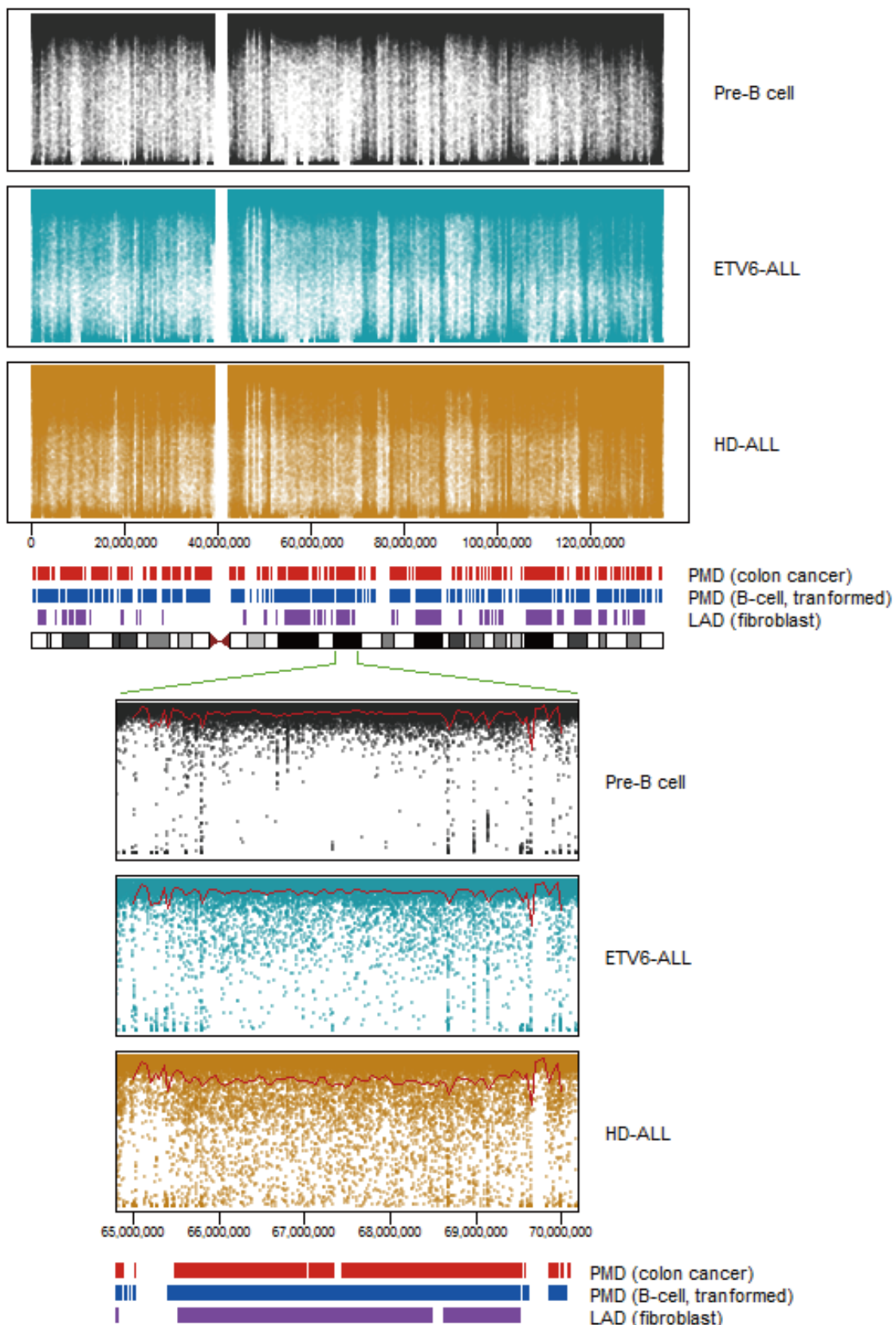


Methylation changes in different functional compartments: WGBS data.

(A) Methylation difference of CpG island (CGI) regions in ETV6-ALL and HD-ALL compared to pre-B cell. ETV6-ALL is more methylated than HD-ALL. The degrees of methylation are similar throughout promoter and gene bodies (approximately +10%) while CGIs in intergenic regions are slightly more methylated.

(B, C) Contour plots show enrichment of *de novo* DMRs (blue) in CGIs in promoters and 5'-bodies due to the dense localization of CGIs in promoter and 5'-body. (B) for ETV6-ALL and (C) for HD-ALL. Profound enrichment of de-DMRs (yellow) is noted upstream regions and outside CGIs.

Supplemental Figure S3

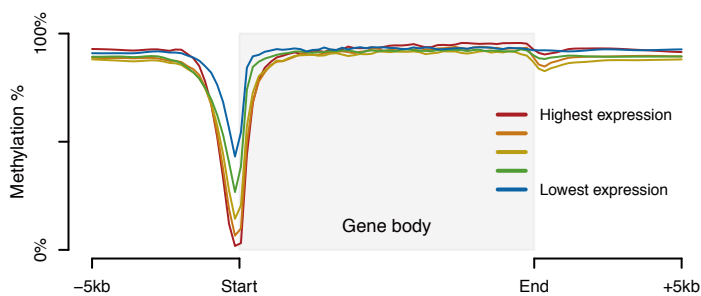


Global overview of an exemplary chromosome (chr10): WGBS data

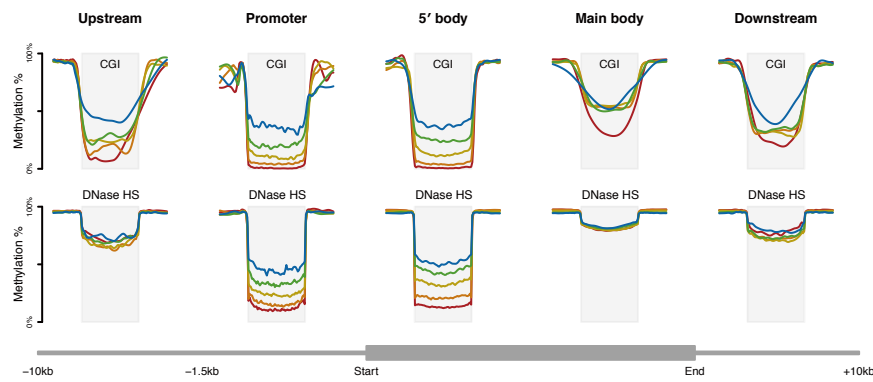
Methylation levels of each CpG were plotted against genomic positions. HD-ALL have large regions with slight demethylation and such regions often coincide with partially methylated domains (PMD) in a colon-cancer cell-line and an EBV-transformed B-lymphoblastoid cell line and lamina-associated domains (LAD) retrieved from a fibroblast. The red lines indicate local regression of average methylation at each position.

Supplemental Figure S4

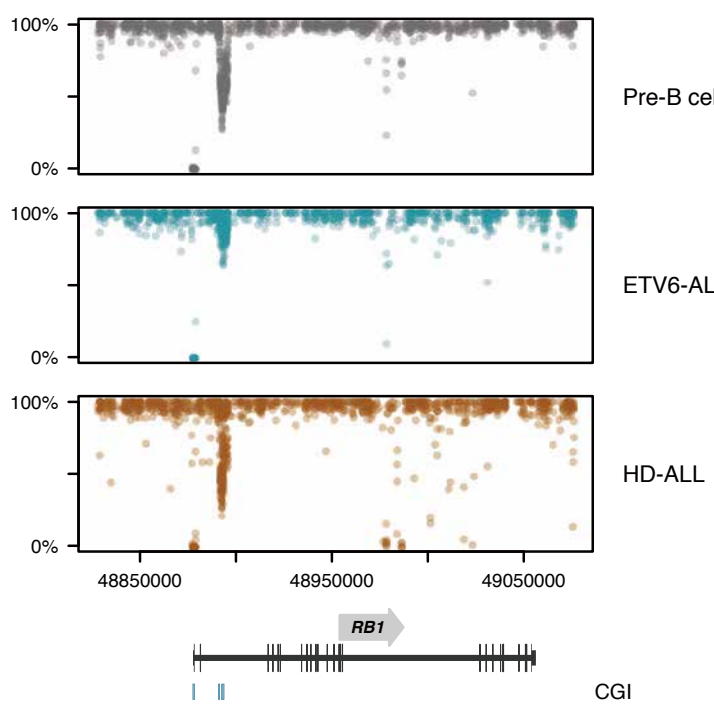
A

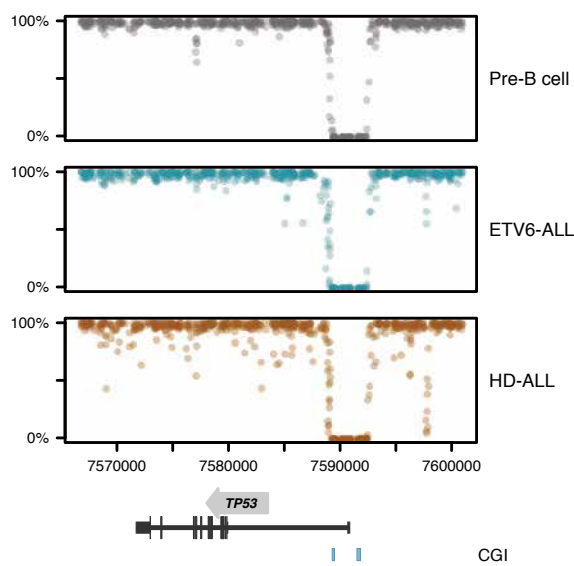
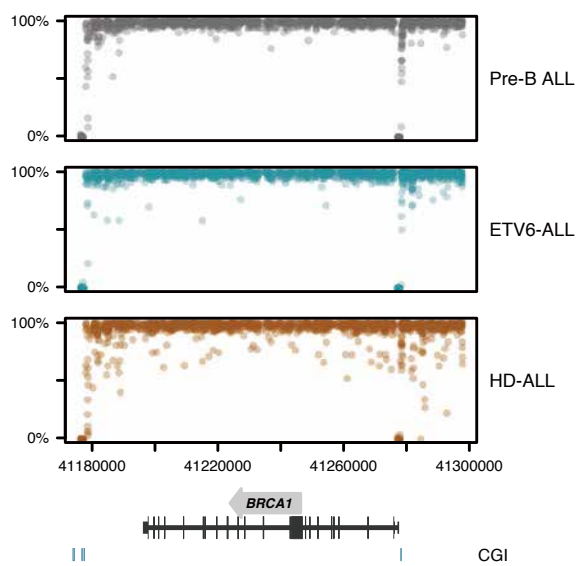
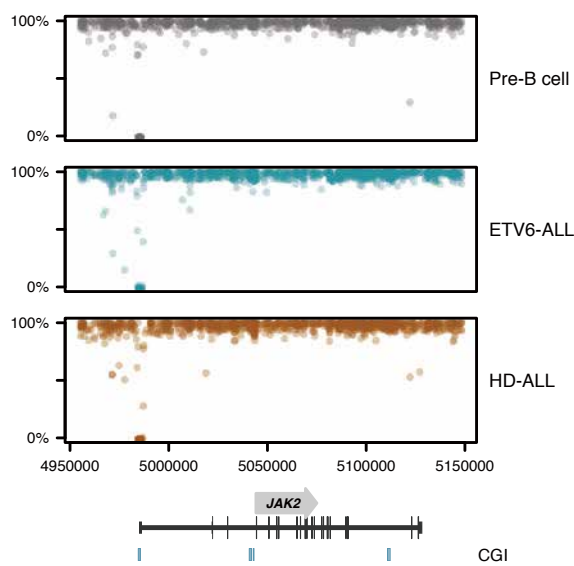
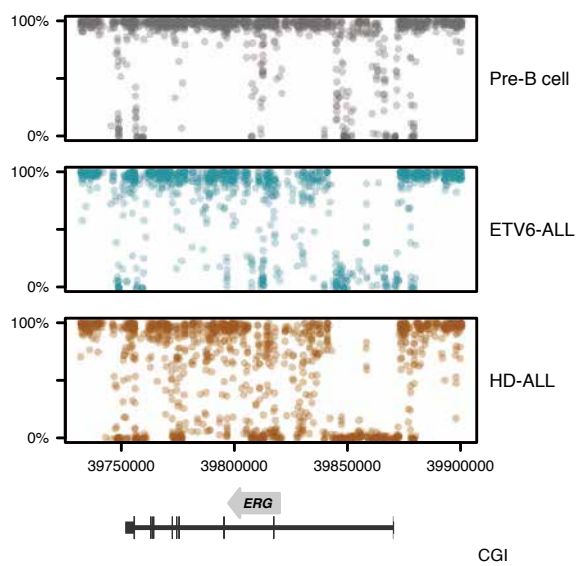


B



C



D**E****F****G**

Association of DNA methylation changes with gene expression: WGBS data.

(A) Association between DNA methylation and gene expression in ETV6-ALL (parallel analysis for HD-ALL is presented in **Fig. 3A-C** of the main paper). Local regression showing methylation levels according to genic locations, stratified by expression quintile. Unlike HD-ALL, slight demethylation of the main body in marginally expressed genes is not observed in ETV6-ALL.

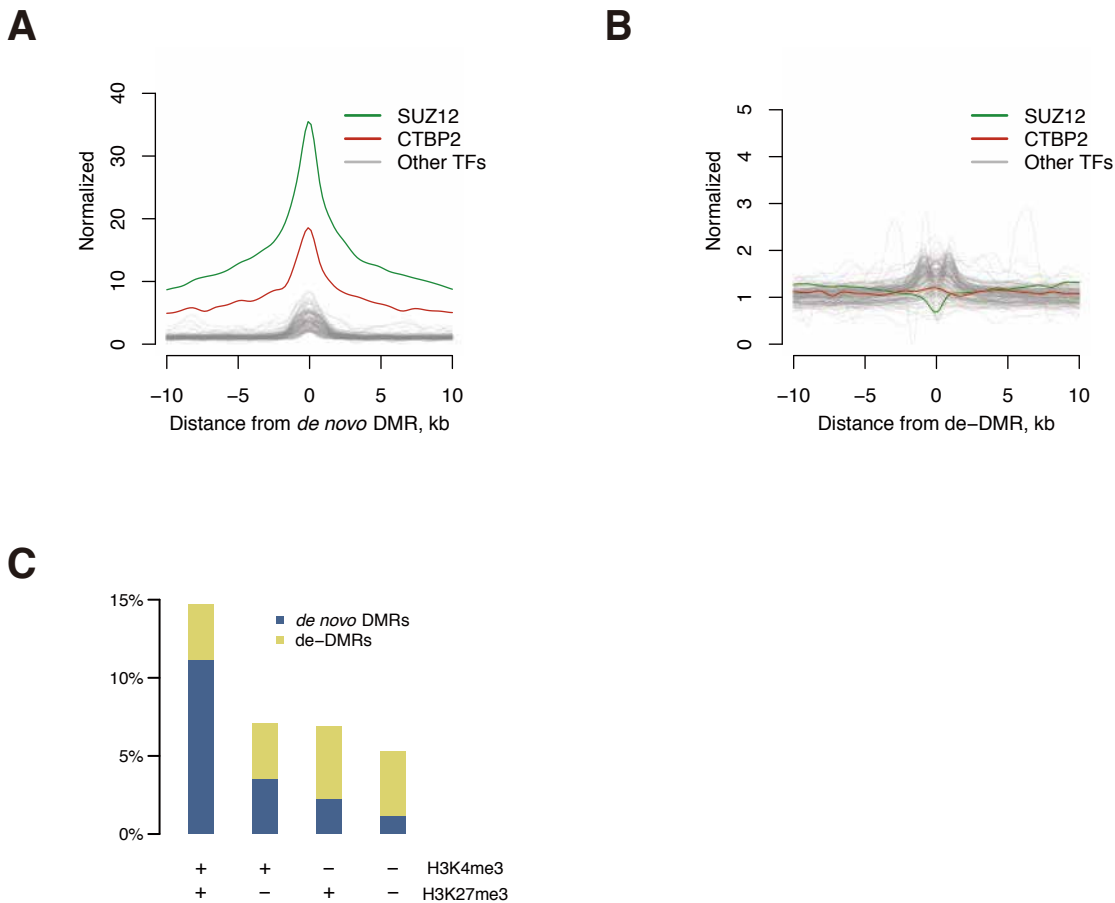
(B) Methylation levels in CGI and DNase HS, stratified by genic location and expression quintile.
 (D) Scatter plot of methylation levels around RB1 shows typical patterns of epigenetic remodeling for gene down-regulation in ETV6-ALL and HD-ALL.

(D, E) Scatter plots of DNA methylation levels around exemplary genes. *TP53* and *BRCA1* are down-regulated both in ETV6-ALL and HD-ALL. HD-ALL has more CpGs demethylated in main body.

(F) *JAK2* is up-regulated and its main body is intact in both B-ALLs.

(G) Both main body and 5'-body of *ERG* are demethylated, but the activating effect of 5'-body demethylation may contribute more and the gene is eventually up-regulated.

Supplemental Figure S5



Enrichment of DMRs of ETV6-ALL according to specific TFs or motifs (parallel analysis for HD-ALL is presented in Fig.4A-C of the main paper): WGBS data.

(A, B) Positional enrichment of *de novo* DMRs and de-DMRs of ETV6-ALL against 148 ENCODE TF-binding sites. Two transcription factors, SUZ12 and CTBP2, are highly enriched around *de novo* DMRs while no specific TFs are enriched around de-DMRs.

(C) Enrichment of DMRs of ETV6-ALL according to H3K4me3 (active) and H3K27me3 (repressive) histone marks of H1 embryonic stem cell (ESC) shows remarkable enrichment of *de novo* DMRs in bivalent domain characterized by co-occupancy of both histone marks.

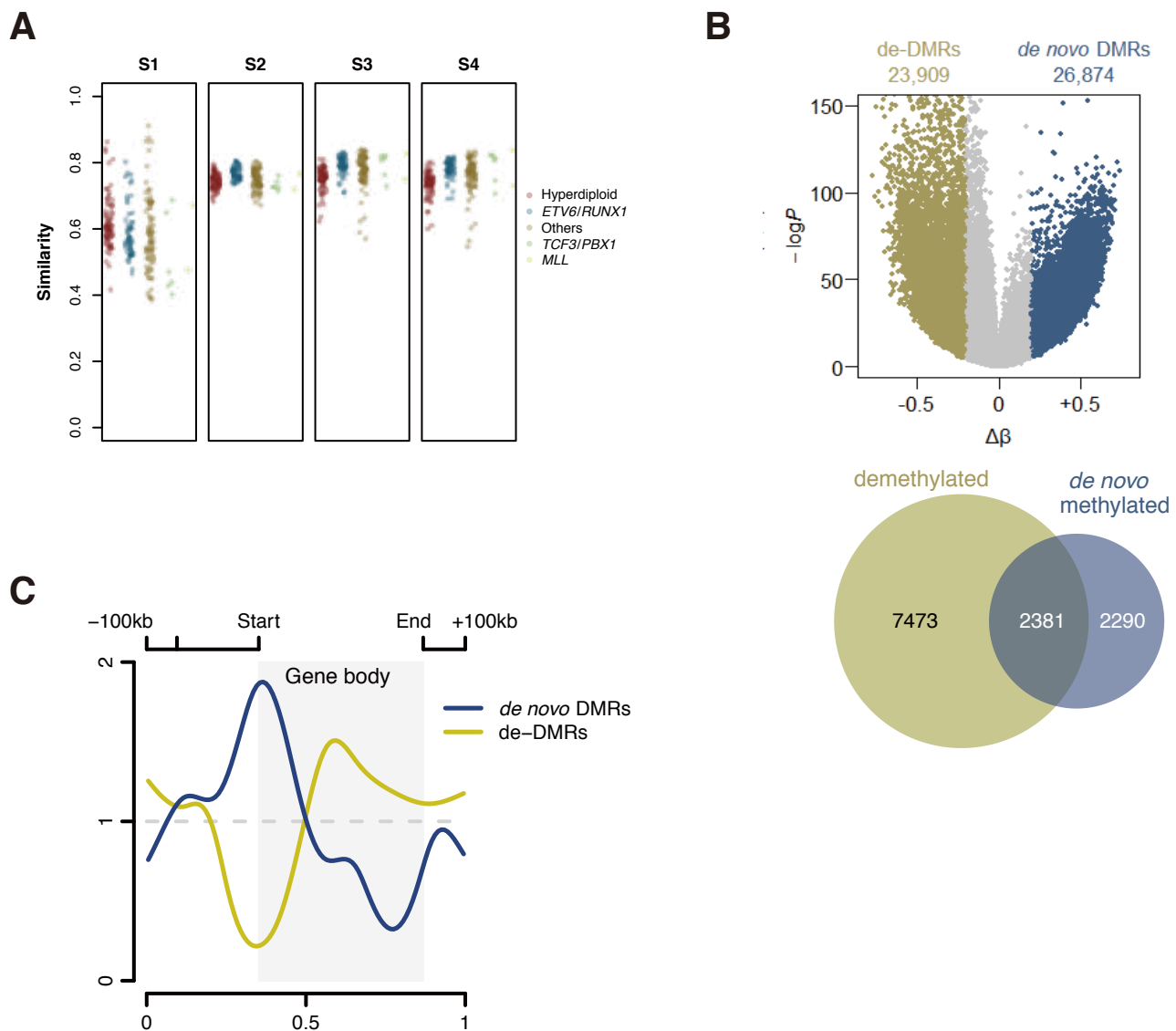
Supplemental Figure S6

	+	-	+	-	H3K4me3 H3K27me3
% of <i>de novo</i> DMRs in specified regions	19.3%	3.6%	4.6%	1.0%	H1-hESC Embryonic stem cells
	15.0%	4.2%	3.9%	1.0%	HUVEC Umbilical vein endothelial cells
	20.2%	3.9%	5.1%	1.1%	HMEC Human mammary epithelial cells
	16.4%	3.1%	4.5%	1.0%	HSMM Normal human skeletal muscle myoblasts
	10.7%	3.0%	3.0%	0.9%	HSMMtube Normal human skeletal muscle myotubes
	15.9%	3.7%	4.2%	1.0%	NH-A Normal human astrocytes
	11.4%	3.6%	3.4%	1.1%	NHDF-Ad Adult normal human dermal fibroblasts
	17.7%	3.9%	3.9%	0.9%	NHEK Epidermal keratinocytes
	12.2%	3.8%	3.9%	1.1%	NHLF Normal human lung fibroblasts
	13.0%	3.5%	4.1%	1.0%	Osteobl Normal human osteoblasts
	7.6%	3.3%	1.8%	1.2%	GM12878 B-cell, EBV transformed
	15.1%	7.1%	2.3%	0.8%	CD14 CD14+ human monocytes
Absolute number of <i>de novo</i> DMRs	177,174	74,471	59,380	178,439	H1-hESC Embryonic stem cells
	78,702	192,196	56,846	161,720	HUVEC Umbilical vein endothelial cells
	69,009	177,245	75,129	168,081	HMEC Human mammary epithelial cells
	103,515	173,883	65,634	146,432	HSMM Normal human skeletal muscle myoblasts
	92,785	222,739	63,432	110,508	HSMMtube Normal human skeletal muscle myotubes
	94,800	182,816	69,078	142,770	NH-A Normal human astrocytes
	76,366	189,540	67,482	156,076	NHDF-Ad Adult normal human dermal fibroblasts
	99,376	182,130	67,644	140,314	NHEK Epidermal keratinocytes
	73,900	192,410	67,768	155,386	NHLF Normal human lung fibroblasts
	85,628	191,754	73,474	138,608	Osteobl Normal human osteoblasts
	67,114	249,626	38,026	134,698	GM12878 B-cell, EBV transformed
	90,821	227,876	41,529	129,238	CD14 CD14+ human monocytes
Numbers of CpGs in specified regions	917,163	2,071,620	1,281,392	17,897,980	H1-hESC Embryonic stem cells
	525,963	4,590,975	1,475,665	15,575,552	HUVEC Umbilical vein endothelial cells
	341,685	4,506,212	1,467,421	15,852,837	HMEC Human mammary epithelial cells
	632,473	5,691,650	1,449,264	14,394,768	HSMM Normal human skeletal muscle myoblasts
	864,584	7,341,964	2,089,115	11,872,492	HSMMtube Normal human skeletal muscle myotubes
	594,637	4,915,105	1,637,870	15,020,543	NH-A Normal human astrocytes
	667,913	5,276,387	1,994,671	14,229,184	NHDF-Ad Adult normal human dermal fibroblasts
	560,038	4,658,288	1,715,521	15,234,308	NHEK Epidermal keratinocytes
	605,279	5,124,365	1,738,403	14,700,108	NHLF Normal human lung fibroblasts
	657,852	5,517,149	1,773,183	14,219,971	Osteobl Normal human osteoblasts
	886,315	7,514,383	2,063,185	11,704,272	GM12878 B-cell, EBV transformed
	600,968	3,197,125	1,794,303	16,575,759	CD14 CD14+ human monocytes

Enrichment of DMRs of ETV6-ALL according to histone marks of different somatic tissues: WGBS data.

From the Broad histone track, we retrieved information on histone marks of different types of somatic tissues. Compared to ESCs, bivalent regions in the somatic cells were much smaller but still showed higher enrichment rates for *de novo* DMRs. The somatic cells had large H3K27me3 domains, and as to absolute numbers, *de novo* DMRs were far more enriched in the H3K27me3 single-occupancy domain.

Supplemental Figure S7

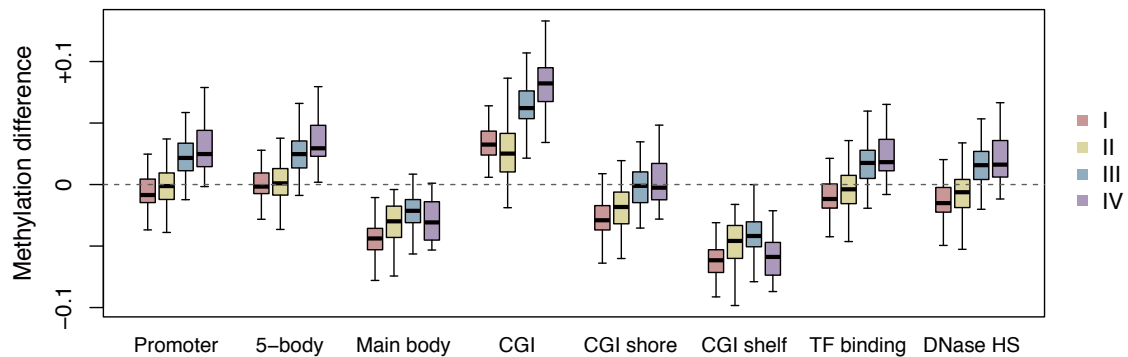


Statistics of methylation HM450 array.

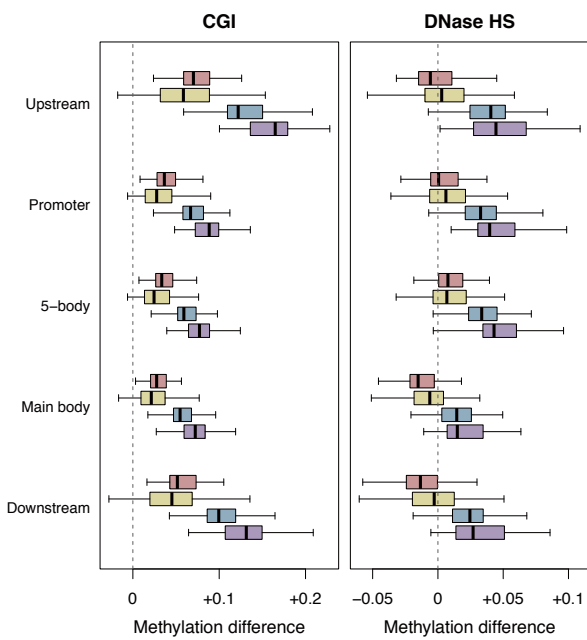
- (A) Similarities of B-ALLs in comparison with different developmental stages of normal B-cells (S1, multipotent progenitors/pro-B cells; S2, pre-B-I cells; S3, pre-B-II cells; S4, immature B cells). Similarity scores were calculated using the Pearson correlation coefficients [$s=(1+r)/2$].
- (B) Overview of DMRs (methylation difference $>20\%$ and FDR-corrected $P<0.01$) of B-ALLs. Volcano plot and Venn diagram showing DMRs compared to normal pre-B cells.
- (C) Relative densities according to locations to gene structure show enrichment of *de novo* DMRs around promoters and de-DMRs around main body.

Supplemental Figure S8

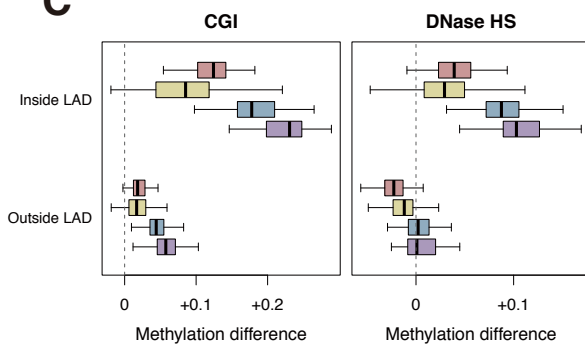
A



B



C



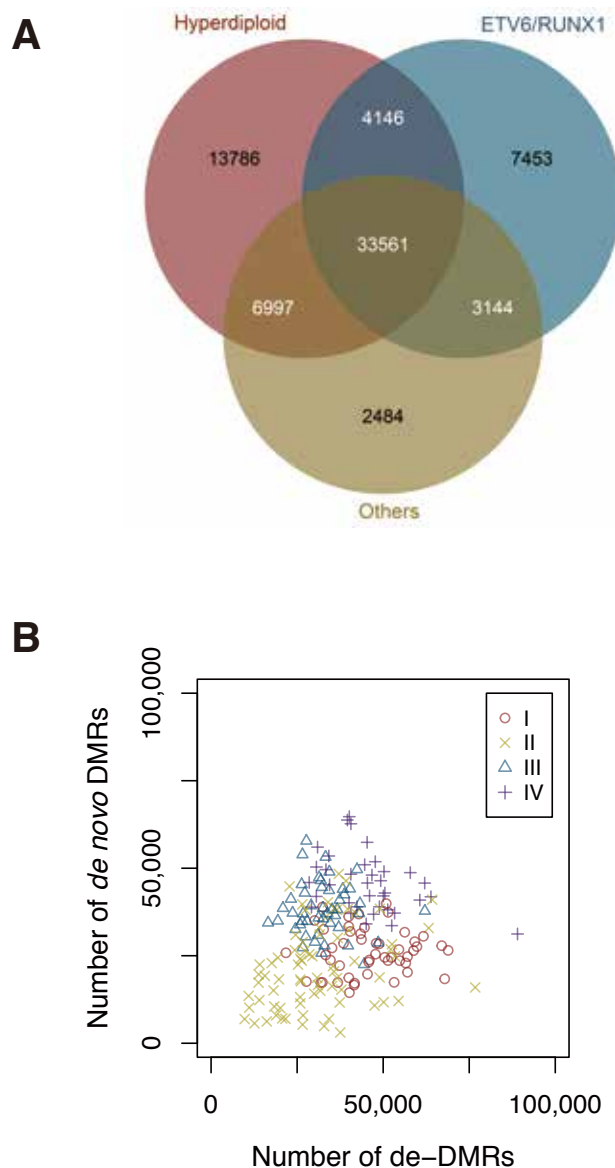
Methylation changes according to specified regions: HM450 array.

(A) In concordance with the findings from WGBS, promoter, 5'-body and CGIs are on average methylated and main body and CGI shelves are demethylated, with different degrees in individual tumors and individual clusters.

(B) CGIs tend to be methylated regardless of the genic location, and DNase HS tend to be more methylated around promoters and the 5'-body, with a wide variability according to each tumor and each cluster.

(C) *De novo* methylation in CGIs and DNase HS are more remarkable in CpGs inside LADs

Supplemental Figure S9

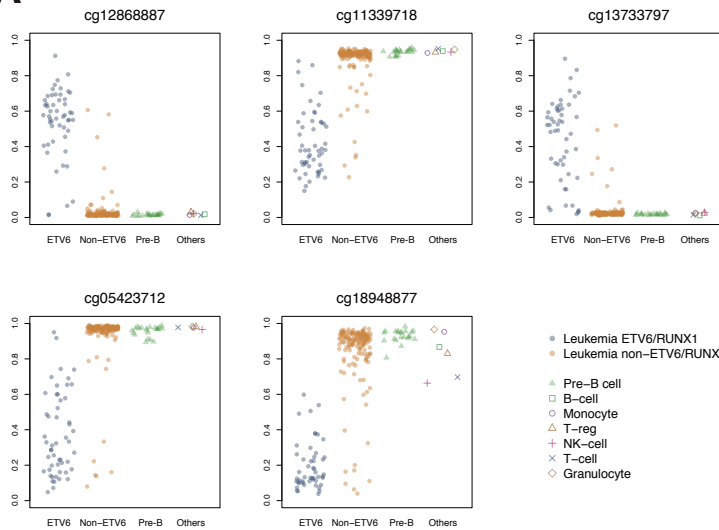


DMRs in each tumor and cytogenetics group: HM450 array.

- (A) Venn diagram showing shared and cytogenetic-specific DMRs. Three cytogenetics groups largely share common DMRs but each also has specific DMRs.
(B) The numbers of DMRs in each tumor varied across broad ranges. Methylation cluster IV had larger numbers of DMRs while cluster II had smaller numbers.

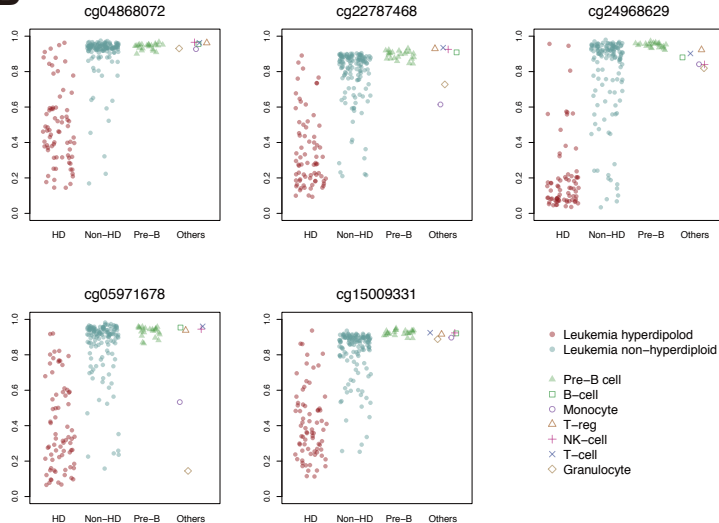
Supplemental Figure S10

A



Illumina probe ID	chrom	position	Nearest gene	Gene location	CGI location	AUC (ROC)	Mean β difference (ETV6 vs non-ETV6)
cg12868887	chr11	70,244,470	<i>CTTN</i>	Promoter	In_CGI	0.972	0.507
cg11339718	chr16	89,000,225	<i>CBFA2T3</i>	Main_body	In_CGI	0.972	-0.467
cg13733797	chr8	121,824,218	<i>SNTB1</i>	5'body	In_CGI	0.969	0.401
cg05423712	chr8	605,100	<i>ERICH1</i>	Downstream	Outside_CGI	0.967	-0.561
cg18948877	chr2	242,904,738	<i>CXXC11</i>	Downstream	Outside_CGI	0.967	-0.644
cg13690063	chr4	40,921,171	<i>AFB2B2</i>	Main_body	Outside_CGI	0.966	-0.463
cg25266281	chr2	242,904,768	<i>CXXC11</i>	Downstream	Outside_CGI	0.966	-0.632
cg07854959	chr17	47,093,489	<i>IGFBP1</i>	Main_body	Shore	0.966	-0.429
cg19093782	chr2	242,904,793	<i>CXXC11</i>	Downstream	Outside_CGI	0.963	-0.496
cg27628854	chr8	121,823,482	<i>SNTB1</i>	5'body	Shore	0.963	0.484
cg06891858	chr18	19,323,333	<i>MIB1</i>	5'body	Shore	0.962	-0.401
cg22295064	chr11	70,244,434	<i>CTTN</i>	Promoter	In_CGI	0.962	0.44
cg14325952	chr8	605,423	<i>ERICH1</i>	Downstream	Outside_CGI	0.962	-0.454
cg18633839	chr18	19,324,759	<i>MIB1</i>	5'body	Shelf	0.961	-0.405
cg02819921	chr2	11,607,488	<i>EF2F6</i>	Promoter	Shore	0.96	-0.504
cg03351491	chr10	134,117,359	<i>STK32C</i>	5'body	Shelf	0.96	-0.472
cg08244848	chr14	34,419,820	<i>EGLN3</i>	5'body	In_CGI	0.96	-0.455
cg22978658	chr11	70,244,453	<i>CTTN</i>	Promoter	In_CGI	0.96	0.441
cg14634687	chr17	47,094,252	<i>IGFBP1</i>	Main_body	Shelf	0.96	-0.424
cg06273125	chr3	113,249,814	<i>SIIT1</i>	Promoter	Shore	0.959	-0.446

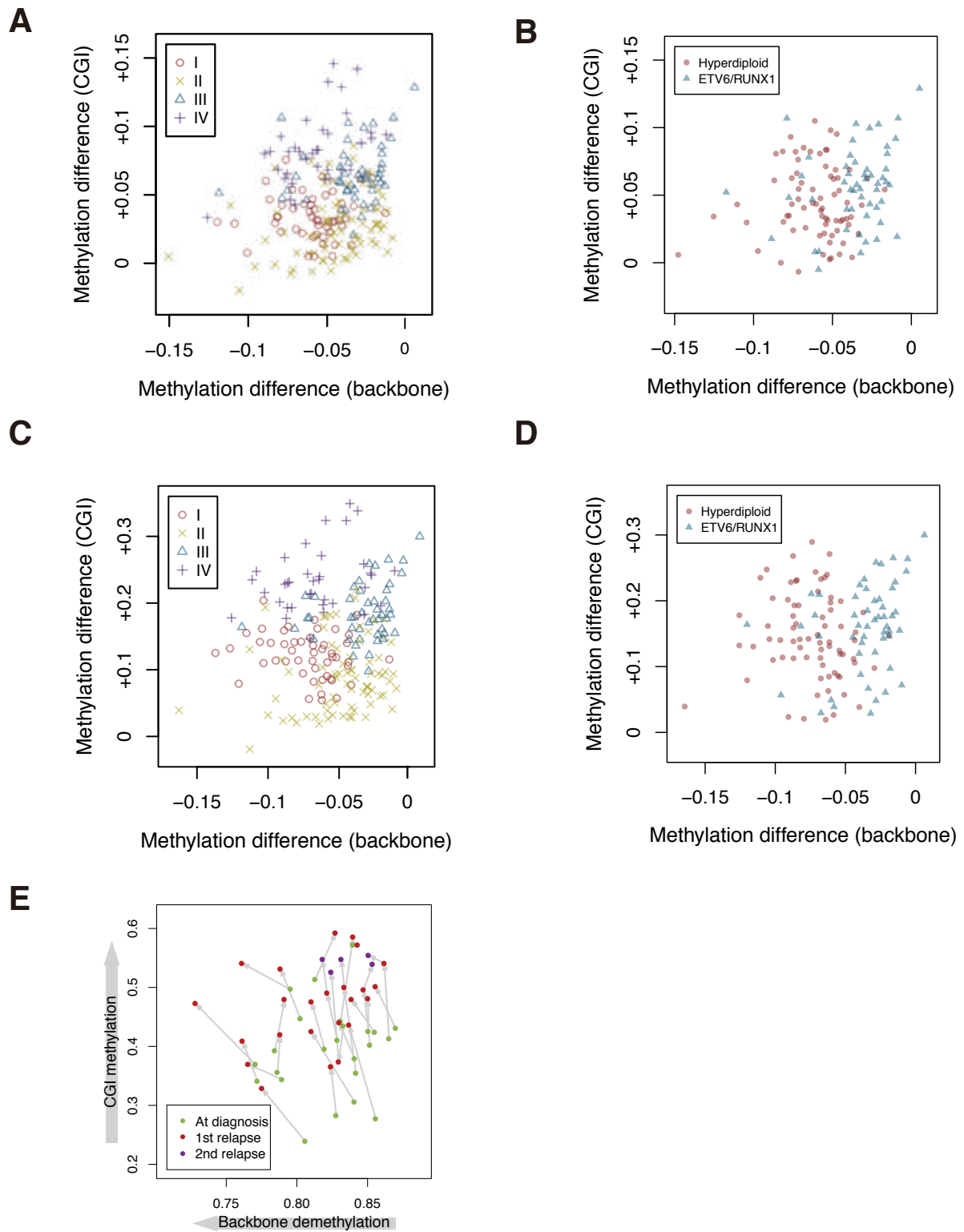
B



Illumina probe ID	chrom	position	Nearest gene	Gene location	CGI location	AUC (ROC)	Mean β difference (HD vs non-HD)
cg04868072	chr16	85,968,253	<i>IRFB</i>	Downstream	Outside_CGI	0.935	-0.411
cg22787468	chr17	27,309,113	<i>SEZ6</i>	Main_body	Shelf	0.931	-0.433
cg24968629	chr22	46,770,644	<i>CELSR1</i>	Main_body	In_CGI	0.931	-0.593
cg05971678	chr10	125,770,089	<i>CHST15</i>	Main_body	Outside_CGI	0.931	-0.458
cg15009331	chr10	80,502,431	<i>ZMIZ1-AS1</i>	Downstream	Outside_CGI	0.93	-0.402
cg12188928	chr17	27,309,139	<i>SEZ6</i>	Main_body	Shelf	0.922	-0.42
cg17832639	chr6	32,078,133	<i>TNXB</i>	Promoter	Outside_CGI	0.919	-0.425
cg14792180	chr5	10,632,056	<i>ANKRD33B</i>	Main_body	Outside_CGI	0.919	-0.408
cg14871313	chr10	7,139,026	<i>SFMBT2</i>	Downstream	Outside_CGI	0.919	-0.43
cg00217055	chr17	76,798,820	<i>USP36</i>	Main_body	Shore	0.918	-0.455
cg14205519	chr9	139,925,750	<i>C9orf139</i>	Main_body	In_CGI	0.916	-0.424
cg13773741	chr17	9,967,499	<i>GAS7</i>	Main_body	Outside_CGI	0.911	-0.448
cg04742550	chr16	31,366,429	<i>ITGAX</i>	Promoter	Outside_CGI	0.908	-0.426
cg02522367	chr9	139,640,325	<i>LCN6</i>	Main_body	Shore	0.908	-0.453
cg17378966	chr5	172,196,746	<i>DUSP1</i>	Main_body	Shore	0.905	0.416
cg02029908	chr5	172,195,602	<i>DUSP1</i>	Main_body	Shore	0.904	0.401
cg00063271	chr17	76,798,776	<i>USP36</i>	Main_body	Shore	0.903	-0.485
cg10113526	chr8	142,163,737	<i>DENND3</i>	Main_body	Outside_CGI	0.902	-0.441
cg18102633	chr19	17,487,776	<i>PLVAP</i>	5'body	Shore	0.902	-0.454
cg13974865	chr21	40,124,308	<i>LINC00114</i>	Main_body	Outside_CGI	0.902	-0.421

Top DMRs discriminating different groups: HM450 array. (A) *ETV6/RUNX1* B-ALLs vs the other B-ALLs. CpGs were ranked according to the area under curve (AUC) values of the receiver-operating characteristic (ROC) analysis, after filtering by methylation difference (>40%). (B) Hyperdiploid B-ALLs vs the other B-ALLs.

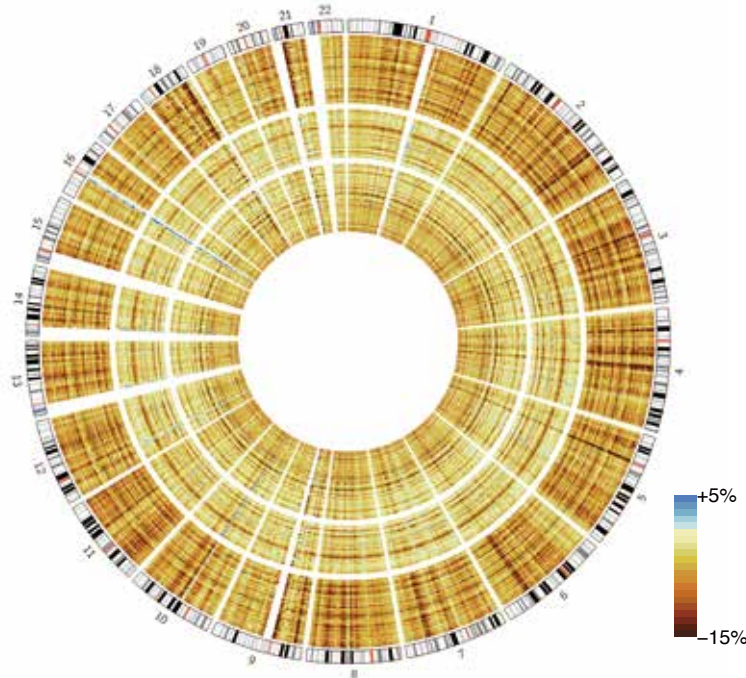
Supplemental Figure S11



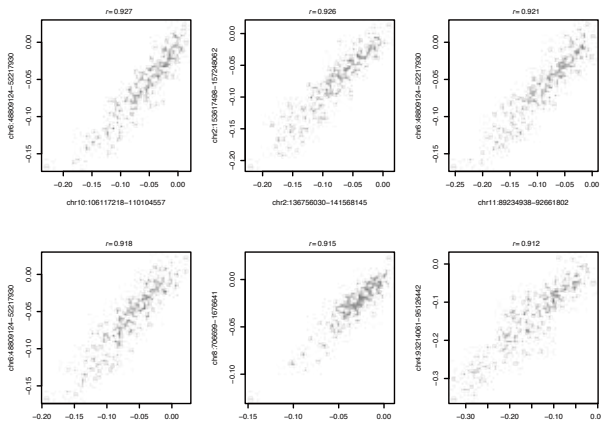
DNA methylation in CGI and backbone regions: HM450 array. (A) Average methylation changes of CGIs and backbones in whole autosomal CpGs in individual cases. Different degrees of methylation changes were noted according to the methylation clusters. (B) Hyperdiploid group shows more demethylation of backbones and is more demethylated than ETV6/RUNX1. (C,D) Parallel analyses using CpGs in LADs show exaggeration of the trend that methylation clusters have different degrees of methylation changes and hyperdiploid have more demethylation. (E) Analysis on an another clinical cohort (Nordlund et al. 2013) illustrates increased CGI methylation and slight backbone demethylation in most relapsed clones.

Supplemental Figure S12

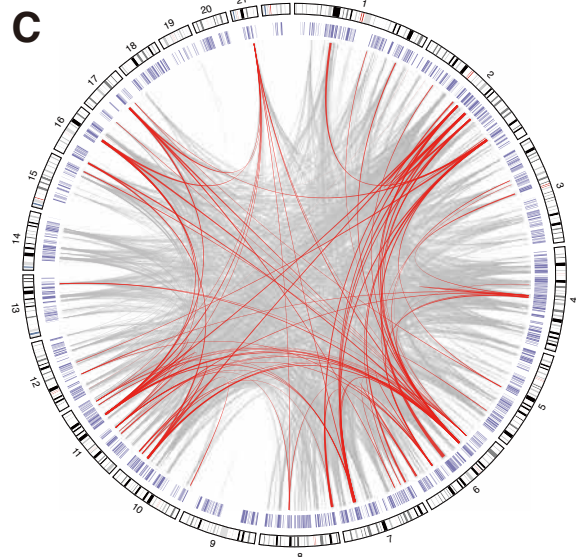
A



B

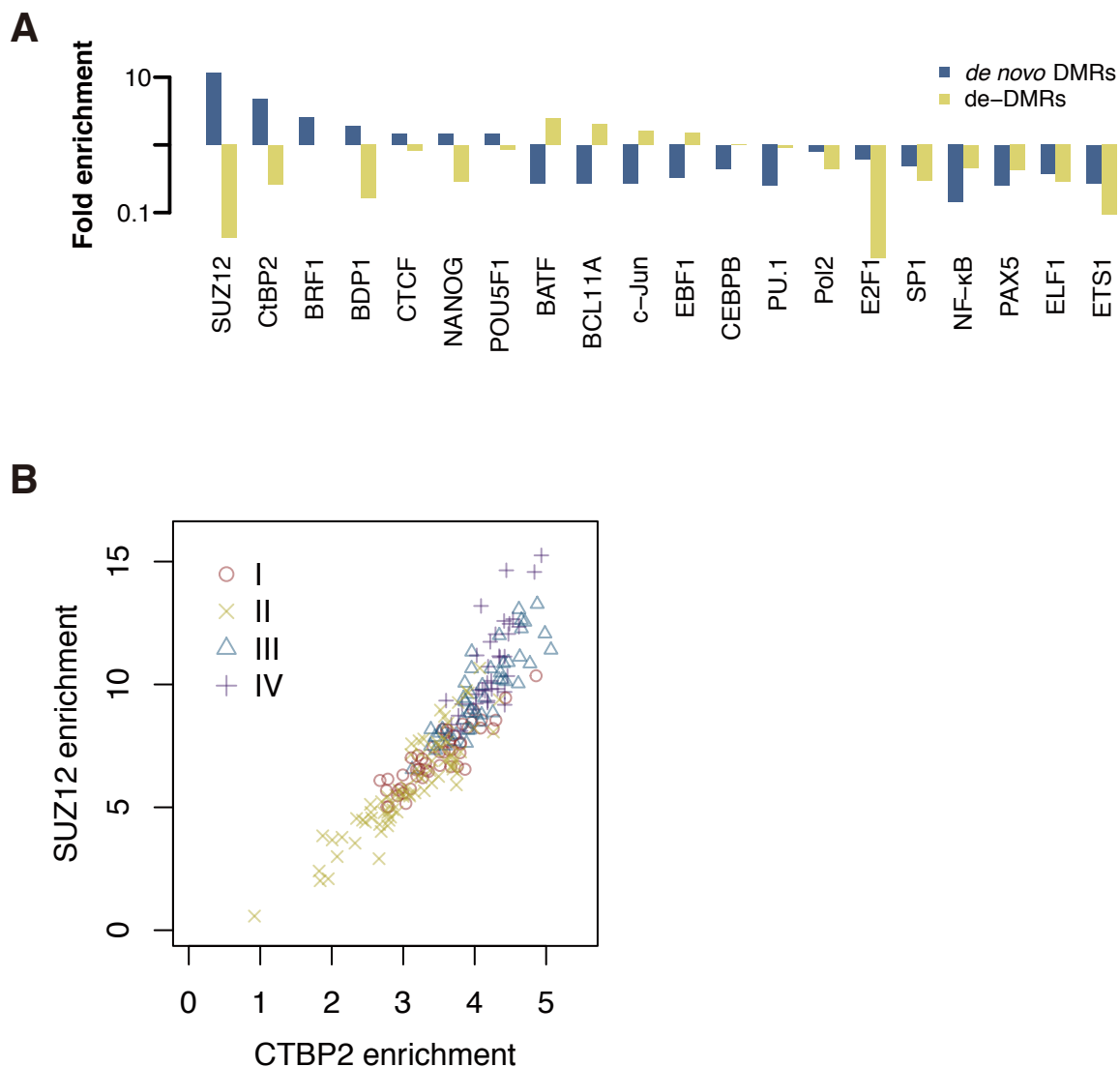


C



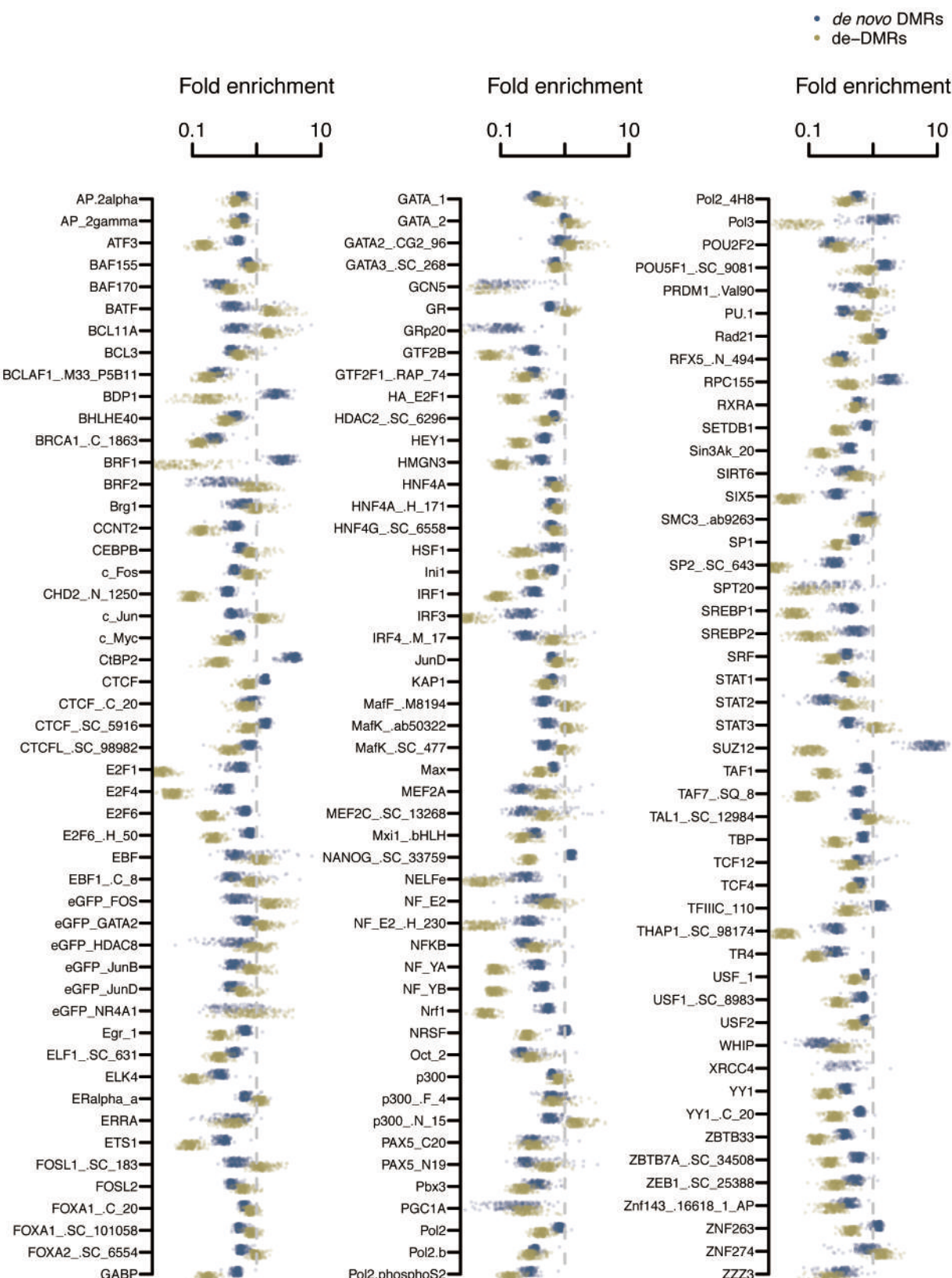
Demethylation of backbones and the correlation of LADs: HM450 array. (A) Circular heatmaps showing methylation changes of backbones across whole genome. From outside to inside, hyperdiploid, ETV6/RUNX1 and other cytogenetics groups are presented. (B) Examples of LADs showing strong correlations of average methylation values with each other. (C) Circular plot showing LADs with strong correlations (red lines for $r > 0.9$ and gray lines for $r > 0.85$). Blue bars indicate LADs.

Supplemental Figure S13



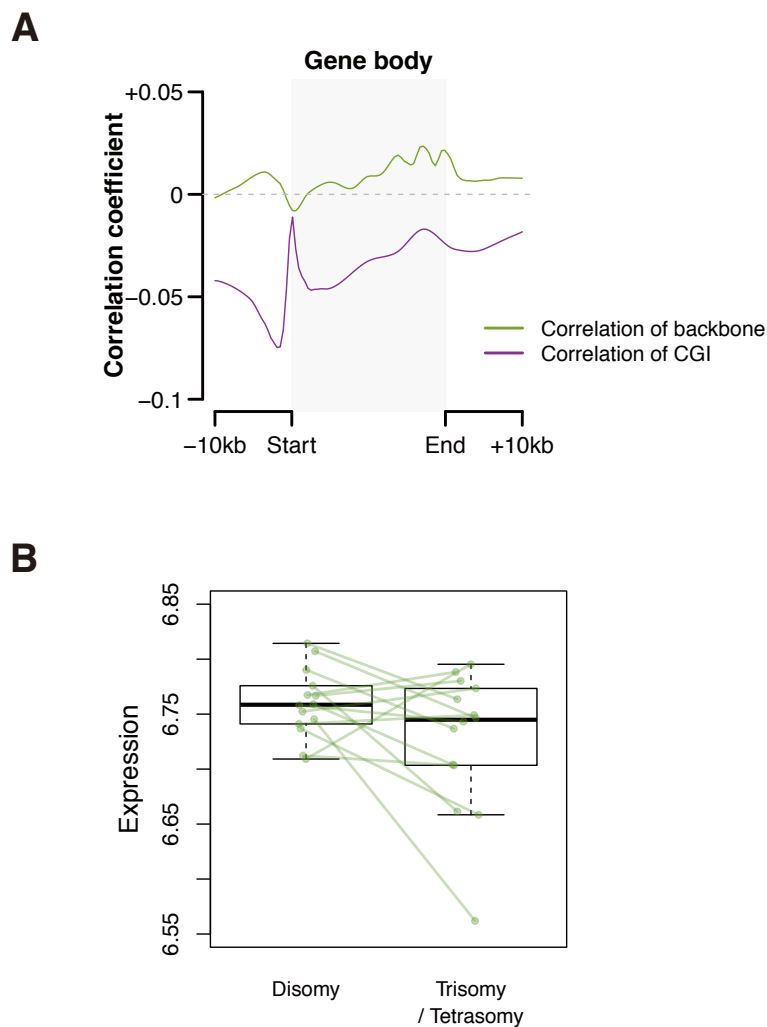
TF enrichment using HM450 array data. (A) Enrichment analysis of DMRs from the HM450 array data against the ENCODE TF tracks showing significant enrichment of SUZ12 and CTBP2. Y-axis is log2-scaled. (B) Enrichment rates of SUZ12 and CTBP in individual tumors illustrate a co-enrichment with higher rates of the clusters III and IV.

Supplemental Figure S14



Enrichment of *de novo* DMRs and de-DMRs of individual tumors against the 148 ENCODE TF binding sites: HM450 array. Y-axis is log2-scaled.

Supplemental Figure S15



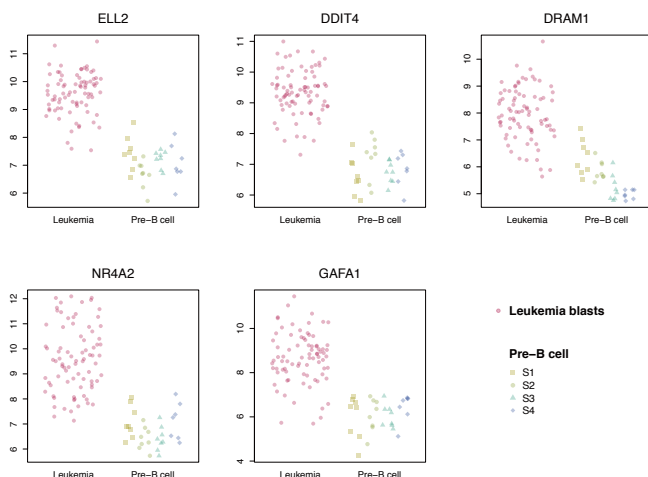
Correlation of expression with genic location and copy numbers: HM450 array and Affymetrix Gene 1.0 ST array data.

(A) As to genic location, CGIs show a strong negative correlation in promoters and backbones show slight positive correlation in the gene's main body. Genes with expression levels (log₂-ratio) >6.0 are selected.

(B) The average expression levels between genes in disomy and trisomy chromosomes, suggesting that different mechanisms besides copy number gain contribute much to gene expression control.

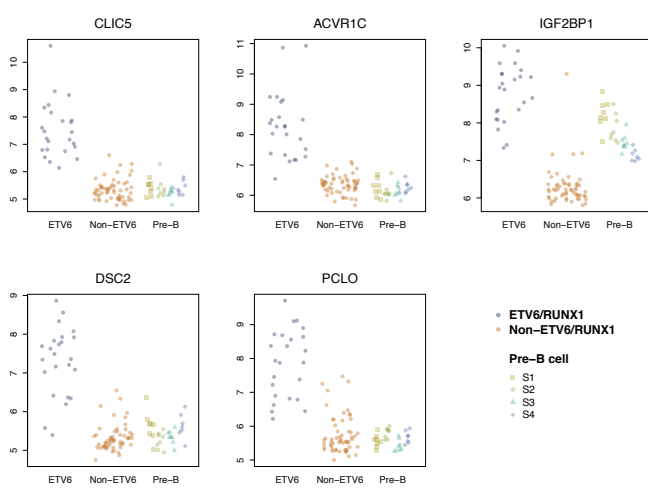
Supplemental Figure S16

A



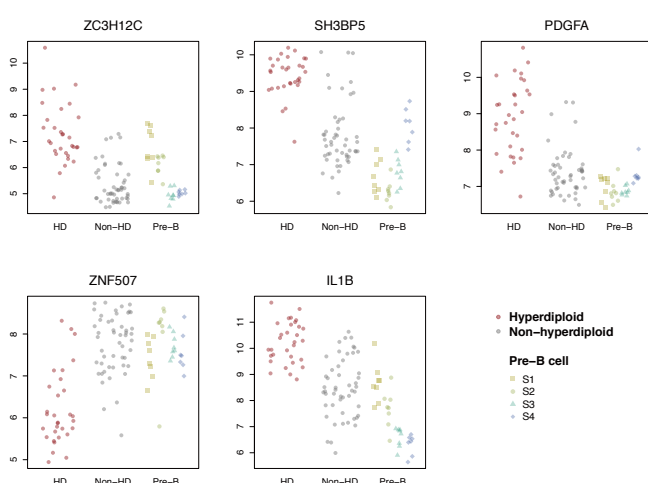
Gene	Expression in B-ALL	Expression in pre-B cell	AUC (ROC)	Mean log2-fold change (B-ALL vs pre-B cell)
<i>ELL2</i>	9.569	7.382	0.957	2.187
<i>DDT4</i>	9.335	7.12	0.953	2.215
<i>TMEM2</i>	9.568	7.564	0.916	2.004
<i>SLC2A3</i>	11.384	8.866	0.915	2.518
<i>HBE GF</i>	10.359	7.974	0.915	2.385
<i>NR4A2</i>	9.598	7.144	0.913	2.454
<i>HBD</i>	9.839	7.444	0.913	2.394
<i>PLIN2</i>	10.102	7.649	0.912	2.453
<i>GAF1</i>	8.665	6.437	0.911	2.228
<i>CA1</i>	8.747	5.911	0.909	2.836
<i>DRAM1</i>	7.974	5.96	0.907	2.014
<i>HBB</i>	12.355	7.127	0.906	5.228
<i>CLEC2B</i>	9.626	7.259	0.906	2.367
<i>RFC1</i>	8.962	6.795	0.903	2.167

B



Gene	Expression in ETV6/RUNX1	Expression in non-ETV6/RUNX1	AUC (ROC)	Mean log2-fold change (ETV6/RUNX1 vs non-ETV6/RUNX1)
<i>CLIC5</i>	7.526	5.336	0.996	2.19
<i>ACVR1C</i>	8.276	6.358	0.992	1.918
<i>IGF2BP1</i>	8.775	6.29	0.987	2.485
<i>DSC2</i>	7.305	5.323	0.98	1.982
<i>PCLO</i>	7.848	5.744	0.969	2.104
<i>FLJ34690</i>	6.642	4.905	0.958	1.737
<i>PTPRK</i>	7.493	5.259	0.957	2.234
<i>FYB</i>	9.782	7.537	0.955	2.245
<i>FYB</i>	10.552	8.007	0.954	2.545
<i>TUSC3</i>	7.755	6.076	0.944	1.678
<i>DSC3</i>	8.468	4.937	0.937	3.531
<i>ENPP4</i>	8.07	6.51	0.937	1.56
<i>CD9</i>	7.935	10.603	0.933	-2.668
<i>NETO1</i>	8.147	5.638	0.93	2.51
<i>GPR110</i>	7.149	5.571	0.925	1.578
<i>NRN1</i>	9.585	6.742	0.92	2.843
<i>MIB1</i>	9.338	7.797	0.917	1.54
<i>TP53INP1</i>	11.359	9.066	0.913	2.293
<i>SH3BP5</i>	7.346	8.88	0.912	-1.534
<i>GBA3</i>	7.159	5.227	0.905	1.932

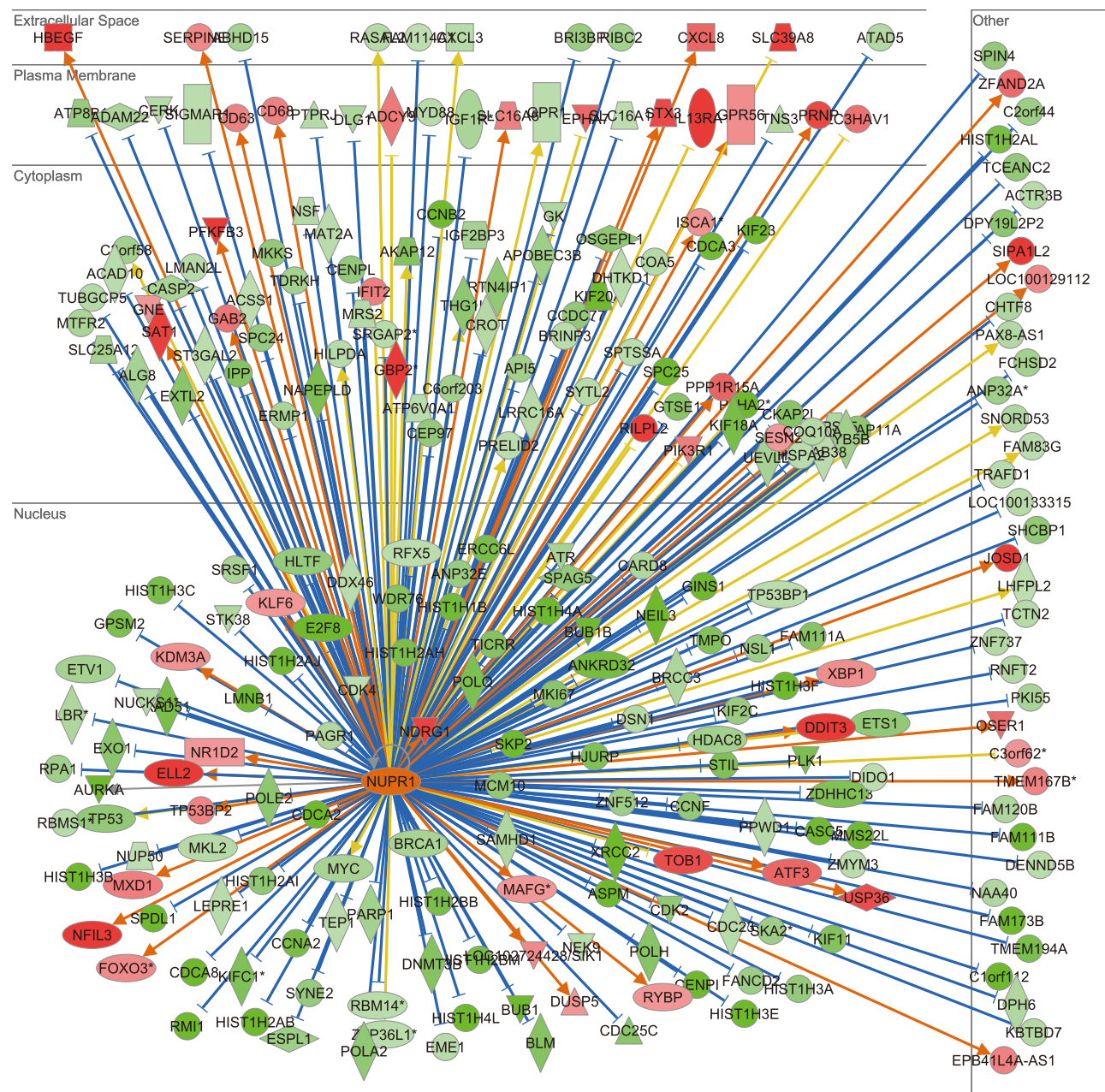
C



Gene	Expression in hyperdiploid	Expression in non-hyperdiploid	AUC (ROC)	Mean log2-fold change (hyperdiploid vs non-hyperdiploid)
<i>ZC3H12C</i>	7.293	5.348	0.926	1.945
<i>SH3BP5</i>	9.427	7.804	0.908	1.622
<i>PDGFA</i>	8.914	7.391	0.899	1.523
<i>ZNF507</i>	6.206	7.762	0.899	-1.556
<i>IL1B</i>	10.213	8.493	0.887	1.72
<i>DDIT4L</i>	10.113	7.43	0.886	2.683
<i>S100A16</i>	10.28	7.397	0.879	2.883
<i>NRN1</i>	6.229	8.424	0.866	-2.195
<i>RAG2</i>	5.115	6.937	0.865	-1.822
<i>IL3RA</i>	9.212	7.692	0.854	1.52
<i>IL3RA</i>	9.212	7.692	0.854	1.52
<i>TP53INP1</i>	8.575	10.472	0.844	-1.897
<i>CD9</i>	10.916	9.128	0.834	1.789
<i>SCN3A</i>	5.163	7.062	0.791	-1.899
<i>SLC10A4</i>	7.45	5.668	0.773	1.782
<i>CLEC4E</i>	7.841	6.058	0.764	1.783
<i>DSC3</i>	4.722	6.765	0.719	-2.043

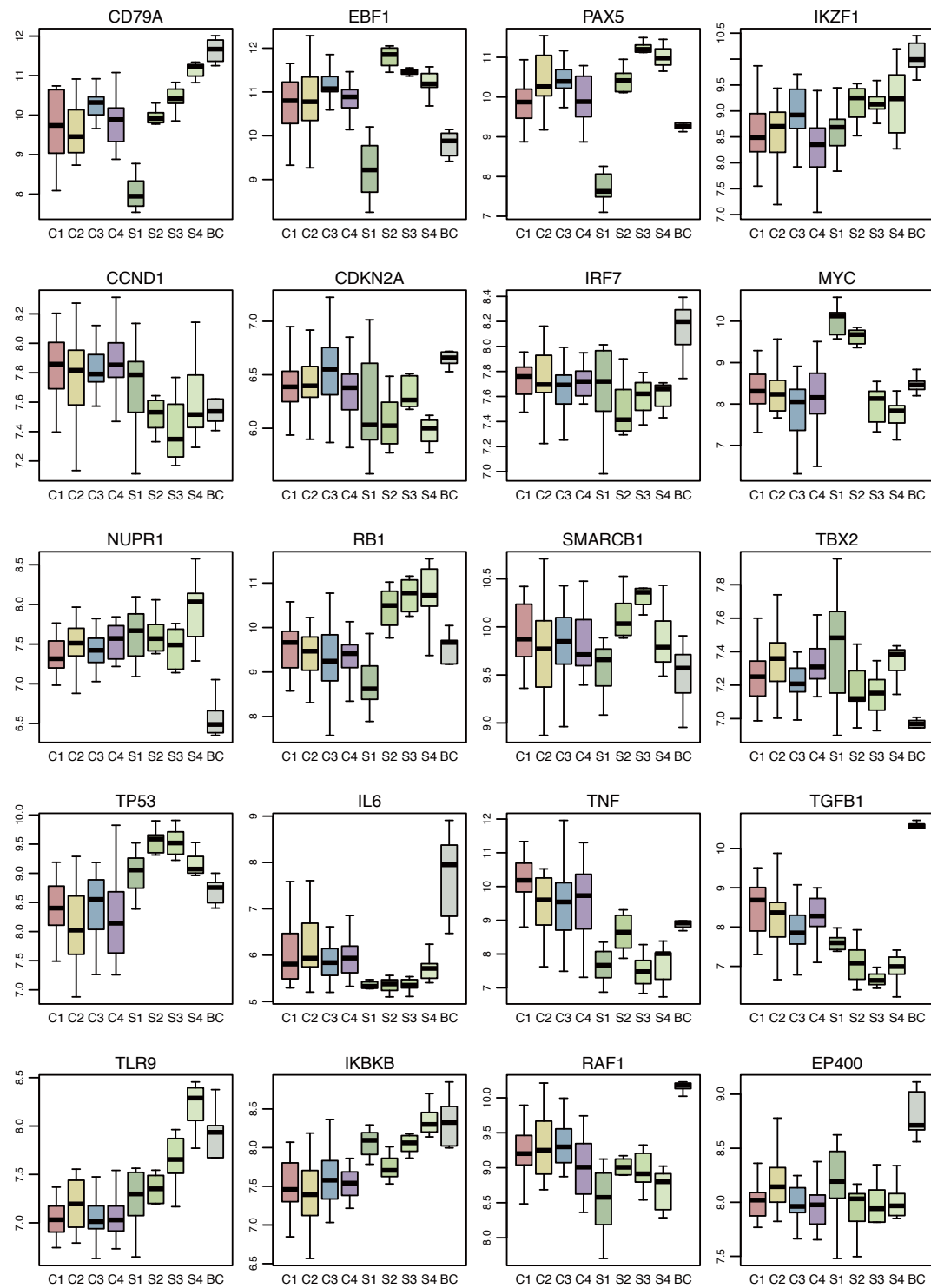
Examples of top genes differentially expressed: Affymetrix Gene 1.0 ST array. (A) DEGs between B-ALLs and normal pre-B cells. Genes were ranked according to the AUC values of the ROC analysis, after filtering by log2-fold difference (>2). (B) DEGs between *ETV6/RUNX1* and the other B-ALLs. Genes were ranked according to the AUC values after filtering by log2-fold difference (>1.5). (C) DEGs between hyperdiploid and the other B-ALLs. Genes were ranked according to the AUC values after filtering by log2-fold difference (>1.5).

Supplemental Figure S17



Example of a significant upstream regulator: Ingenuity Pathway Analysis results from the Affymetrix Gene 1.0 ST array data. NUPR1 is a transcription factor with the highest activation z score with P-values $<1.0 \times 10^{-40}$. Most target genes previously known to be suppressed by NUPR1 are down-regulated and most genes known to be activated by NUPR1 are up-regulated, suggesting the activity of NUPR1 is increased in tumor cells.

Supplemental Figure S18



Expression levels of key developmental genes and significant regulators: Affymetrix Gene 1.0 ST array data.

Expression levels of methylation clusters and control B-cells according to maturation stages (S1, multipotent progenitors/pro-B cells; S2, pre-B-I cells; S3, pre-B-II cells; S4, immature B cells; BC, mature peripheral B-cells). Most B-ALLs are previously known to be close to S2 and S3, as exemplified by CD79A. However, different degrees of dysregulation is noted in different genes which dynamically change during normal development.

Supplemental Figure S19

Upstream regulator	I					II					III					IV					Type
	S1	S2	S3	S4	BC	S1	S2	S3	S4	BC	S1	S2	S3	S4	BC	S1	S2	S3	S4	BC	
CCND1	-3.1	-5.0	-4.3	2.0	3.9	-3.9	-5.2	-4.8	n.s.	2.6	-1.8	-4.7	-4.4	3.0	3.8	-2.9	-4.8	-3.8	2.5	4.4	transcription regulator
CDKN2A	4.2	5.0	5.3	-0.7	-3.1	5.2	6.0	5.9	0.5	-3.9	3.6	5.4	5.4	-3.0	-4.3	4.5	5.5	5.3	-0.7	-3.7	transcription regulator
HIF1A	3.5	3.7	3.2	4.0	-3.9	3.1	2.8	2.3	3.2	-5.2	2.3	3.3	2.9	3.9	-4.4	2.5	2.9	2.2	3.3	-4.5	transcription regulator
IRF7	6.2	5.1	4.3	4.1	-1.2	5.6	4.3	3.5	3.6	-1.5	6.3	5.7	4.1	3.9	-1.4	5.6	4.5	3.8	3.5	-1.2	transcription regulator
MYC	-3.6	-5.6	-4.2	2.6	4.2	-4.0	-6.0	-4.0	2.2	4.6	-2.9	-5.0	-3.0	4.0	4.8	-4.1	-5.9	-3.4	3.4	5.3	transcription regulator
NUPR1	8.1	11.4	12.1	6.5	-5.6	8.9	10.8	12.5	7.4	-4.9	4.7	8.8	10.4	2.4	-7.0	7.8	11.1	11.6	5.3	-5.5	transcription regulator
RB1	4.6	4.8	5.3	0.9	-2.3	4.3	4.3	5.0	1.8	-2.2	4.2	4.8	4.8	-0.8	-2.0	4.6	4.9	5.5	1.2	-2.3	transcription regulator
RELA	3.3	4.5	4.4	3.2	-4.8	2.3	4.0	4.1	2.9	-5.2	2.3	4.2	4.2	2.6	-5.6	2.6	4.7	4.3	2.6	-4.6	transcription regulator
SMARCB1	3.4	5.1	4.6	n.s.	-3.5	3.4	4.5	4.3	1.6	-4.2	3.1	4.7	3.9	0.2	-3.0	3.6	4.6	4.0	1.0	-3.6	transcription regulator
STAT4	4.6	4.5	4.6	6.2	-3.4	3.2	3.5	3.1	5.6	-4.1	3.9	4.4	3.9	5.9	-3.3	3.8	3.9	3.5	6.1	-3.9	transcription regulator
TBX2	-5.2	-5.6	-5.4	n.s.	-4.5	-5.7	-6.1	-5.3	-0.7	4.5	-4.4	-5.6	-5.4	3.0	5.1	-4.8	-5.4	-5.0	0.8	4.5	transcription regulator
TP53	5.2	5.8	5.2	3.6	-4.4	5.4	5.7	5.4	4.5	-5.1	5.1	6.1	5.6	1.7	-5.3	5.1	6.2	5.6	2.8	-4.9	transcription regulator
XBP1	1.8	1.4	2.5	3.3	-4.6	2.0	2.2	1.7	2.8	-5.0	1.5	1.9	1.2	2.9	-4.5	0.3	0.6	1.0	1.7	-4.5	transcription regulator
IFNA2	6.3	5.3	5.6	4.7	-1.6	6.1	4.8	5.1	4.4	-2.5	5.8	4.9	4.7	4.4	-2.2	6.1	4.0	4.6	3.8	-1.7	cytokine
IFNB1	5.4	3.9	2.7	2.3	0.9	5.6	4.2	2.3	1.1	0.8	5.4	4.2	2.3	1.5	0.6	4.7	2.6	2.1	0.9	0.5	cytokine
IFNG	7.3	8.0	7.0	5.4	-6.5	5.5	5.2	5.6	4.5	-7.8	6.5	6.8	5.9	4.4	-6.9	6.4	6.5	6.0	4.7	-6.5	cytokine
IFNL1	5.4	5.1	4.6	4.1	0.5	5.6	4.5	4.0	3.7	n.s.	5.7	5.0	4.3	3.5	-0.3	5.0	4.3	4.1	3.4	n.s.	cytokine
IL1A	4.0	5.5	4.9	3.9	-4.4	3.3	4.4	5.2	3.0	-5.0	3.2	4.1	4.7	2.1	-5.8	3.6	4.7	5.0	3.3	-4.4	cytokine
IL1B	5.5	7.1	7.0	5.9	-7.5	4.5	6.3	6.9	6.6	-7.7	3.5	6.4	7.0	4.9	-8.4	4.8	6.2	6.7	5.4	-7.6	cytokine
IL1RN	-4.9	-5.1	-4.0	-3.2	n.s.	-5.4	-4.9	-3.7	-3.0	2.5	-5.0	-5.2	-3.9	-2.8	2.2	-4.8	-4.4	-3.5	-3.3	n.s.	cytokine
IL2	3.3	4.5	5.6	5.5	-4.8	2.0	3.5	4.5	5.2	-4.2	1.7	3.6	4.6	5.1	-4.8	1.9	3.5	4.6	5.1	-4.9	cytokine
IL4	2.3	2.4	2.1	3.3	-4.8	0.9	0.7	0.3	1.0	-4.9	0.7	1.9	1.1	1.7	-4.6	2.1	1.4	1.0	2.0	-5.1	cytokine
IL5	4.7	4.6	4.5	5.1	-4.6	3.2	3.3	3.3	5.1	-5.6	2.7	5.0	4.2	4.6	-5.6	4.0	4.0	4.1	5.2	-5.1	cytokine
IL6	4.3	5.5	5.0	4.9	-5.8	3.7	4.3	4.8	3.9	-6.3	4.2	5.5	4.8	3.9	-6.4	3.3	3.8	4.3	4.0	-6.3	cytokine
OSM	4.4	5.2	4.0	2.8	-3.3	4.4	5.0	3.6	2.1	-3.6	4.2	5.2	4.6	2.3	-3.2	3.9	4.4	2.8	2.0	-3.4	cytokine
TNF	7.6	8.6	6.7	5.7	-8.3	6.7	6.8	5.8	5.1	-8.8	6.2	7.2	5.9	3.7	-9.1	6.9	7.0	5.8	4.0	-8.8	cytokine
TNFSF11	3.0	3.5	3.4	4.2	-4.7	1.2	2.7	2.5	3.3	-5.4	1.6	2.5	2.3	3.3	-5.5	2.1	2.6	2.3	3.0	-5.2	cytokine
EGF	2.4	4.0	4.1	5.8	-3.4	2.4	3.3	3.8	5.2	-3.1	1.4	2.7	2.9	4.5	-4.8	2.2	3.9	3.6	5.1	-3.8	growth factor
HGF	1.1	-0.9	-0.5	4.8	-1.2	-0.7	-1.4	-1.2	3.3	-1.8	1.2	-1.2	-0.9	5.1	-1.6	0.6	-1.2	-1.5	4.0	-1.9	growth factor
TGFB1	3.8	4.6	4.5	5.6	-5.3	2.3	4.1	4.7	4.7	-5.6	2.2	3.4	3.6	4.2	-5.9	2.5	3.9	4.5	3.9	-6.2	growth factor
TLR3	5.5	6.2	6.0	5.2	-2.7	5.2	5.9	6.3	5.3	-3.4	4.4	5.7	4.6	3.7	-3.9	4.8	5.6	5.9	4.7	-3.0	transmembrane receptor
TLR4	4.6	5.7	6.3	6.1	-4.0	3.1	3.7	5.0	4.9	-4.6	3.4	4.4	5.7	4.9	-4.3	4.5	4.4	5.4	5.1	-4.1	transmembrane receptor
TLR9	4.5	5.6	5.4	4.9	-2.1	3.9	5.3	5.7	5.2	-3.0	3.1	4.8	4.0	3.3	-3.7	3.8	4.9	5.5	4.3	-2.2	transmembrane receptor
IKBKB	3.2	5.2	5.2	3.4	-3.7	2.6	4.9	4.3	1.9	-3.8	2.5	4.7	4.0	1.6	-4.4	3.3	4.9	4.5	2.4	-3.4	kinase
RAF1	4.2	4.8	4.5	5.4	-2.7	2.5	4.3	4.5	5.0	-3.4	2.2	3.1	3.7	4.6	-3.4	3.4	3.7	3.4	4.4	-2.9	kinase
SYVN1	2.5	1.7	2.3	3.8	-4.6	0.6	0.7	1.4	3.8	-5.1	2.1	1.6	2.0	4.6	-4.6	1.6	1.0	1.2	4.0	-4.6	transporter
TGM2	4.6	5.9	5.5	2.4	-5.3	5.4	5.7	5.6	2.6	-6.6	4.7	5.4	5.5	2.5	-6.7	4.9	5.1	4.7	2.2	-6.2	enzyme
F2	2.5	4.0	3.0	4.0	-5.1	1.2	3.7	3.7	3.7	-5.7	1.0	3.2	3.1	3.4	-5.8	2.1	3.1	3.0	3.7	-5.5	peptidase
(NFkB (complex))	5.1	6.7	7.1	6.5	-6.7	4.6	5.5	6.0	5.7	-7.7	3.9	6.3	6.3	5.1	-8.0	4.6	5.9	6.0	5.7	-6.8	complex
PDGF BB	4.3	5.9	6.1	5.6	-4.7	3.2	5.3	5.7	4.1	-6.1	2.8	4.4	4.2	4.2	-5.8	3.8	5.3	5.5	4.6	-5.5	complex
CD3	-3.9	-2.8	-3.2	-5.2	2.6	-1.4	-0.5	-1.4	-4.5	3.4	-1.6	-0.9	-2.2	-4.3	3.3	-2.9	-0.6	-2.4	-4.8	3.1	complex
ERK	2.3	3.3	3.7	2.9	-4.8	2.6	3.6	3.6	3.9	-4.7	1.1	3.0	2.5	2.8	-5.3	1.7	3.2	3.4	2.6	-4.8	group
IFN Beta	5.1	3.8	3.3	3.3	-0.3	4.6	3.2	2.9	2.5	-1.3	4.5	3.7	2.9	2.6	-1.0	4.3	2.6	2.7	2.5	-0.7	group
IL1	3.3	4.9	5.5	4.3	-4.8	2.1	3.8	5.1	3.8	-5.1	0.0	3.9	4.2	2.2	-5.6	2.0	3.8	4.8	3.5	-4.9	group
Interferon alpha	6.9	6.8	5.4	4.6	-3.7	6.0	5.6	4.2	3.7	-3.8	6.1	5.6	4.2	3.2	-4.0	5.9	4.6	4.2	3.0	-3.7	group
Vegf	1.3	-0.6	-0.3	4.8	-2.5	-0.4	-0.8	-0.9	3.9	-2.5	0.9	-0.8	-0.4	5.3	-2.7	0.6	-1.3	-0.9	3.9	-2.8	group
EP400	-3.2	-5.1	-5.0	n.s.	4.1	-3.7	-5.2	-5.0	n.s.	3.7	-2.4	-5.1	-4.8	n.s.	4.5	-3.1	-5.1	-4.9	n.s.	4.1	other
INSIG1	-2.0	-2.5	-3.9	-3.5	4.2	-1.7	-2.0	-4.1	-2.7	4.9	0.0	-2.0	-2.3	n.s.	5.2	-1.9	-2.7	-4.1	-4.0	4.3	other
MYD88	2.2	4.4	4.3	3.4	-5.1	2.3	3.8	4.3	4.1	-5.2	2.0	4.3	3.5	3.2	-5.8	2.1	3.6	4.3	3.6	-5.6	other
miR-1 (GGAAUGU)	-1.4	n.s.	0.7	n.s.	4.4	-1.4	0.5	n.s.	-2.9	4.2	n.s.	n.s.	n.s.	n.s.	3.9	-1.3	n.s.	1.5	-2.6	5.0	mature microRNA
miR-124-3p (AAGGCAC)	-2.3	-1.1	-1.4	-4.7	5.2	-0.4	0.1	0.3	-2.7	6.4	-2.3	-0.2	0.1	-3.9	5.3	-1.7	0.1	0.2	-3.8	5.5	mature microRNA
prostaglandin E2	1.0	1.9	1.9	0.6	-4.6	1.0	2.5	2.4	2.0	-4.3	1.1	3.0	2.6	n.s.	-4.5	0.5	1.7	1.5	0.3	-5.0	chemical - endogenous
tretinoin	6.9	5.9	4.4	1.6	-6.2	5.9	5.9	4.7	1.9	-6.5	5.9	6.0	4.7	1.4	-6.9	5.9	6.1	4.2	1.2	-6.1	chemical - endogenous
uric acid	3.2	5.0	5.5	2.4	-2.6	3.6	4.9	5.8	3.5	-3.3	1.9	3.7	4.7	0.7	-3.5	3.4	4.9	5.3	2.5	-2.8	chemical - endogenous
LY294002	-3.6	-3.0	-2.8	-4.9	4.8	-3.2	-3.0	-2.4	-4.2	5.3	-2.7	-3.0	-1.8	-3.9	5.4	-3.3	-2.7	-2.1	-4.3	5.3	chemical - kinase inhibitor
PD98059	-3.6	-4.4	-4.6	-6.4	3.7	-2.1	-3.8	-3.9	-5.8	4.0	-1.9	-3.3	-4.3	-5.3	4.4	-3.1	-3.9	-3.9	-6.1	3.6	chemical - kinase inhibitor
SB203580	-4.8	-5.7	-7.0	-5.8	4.6	-3.7	-5.6	-6.4	-4.9	5.5	-2.9	-5.1	-6.0	-4.1	5.5	-4.7	-5.7	-6.8	-5.2	4.3	chemical - kinase inhibitor
SP600125	-3.1	-5.0	-5.5	-3.3	3.2	-2.2	-5.2	-5.5	-4.1	3.6	n.s.	-4.5	-4.7	-2.0	4.0	-2					